AD-A141 533 OVERVIEW OF ULTRAVIOLET REMOTE SENSING OF THE IONOSPHERE(U) NAVAL RESEARCH LAB WASHINGTON DC R R MEIER 12 APR 84 NRL-MR-5292 SBI-AD-E000 567 1/1

UNCLASSIFIED F/G 17/5 NL

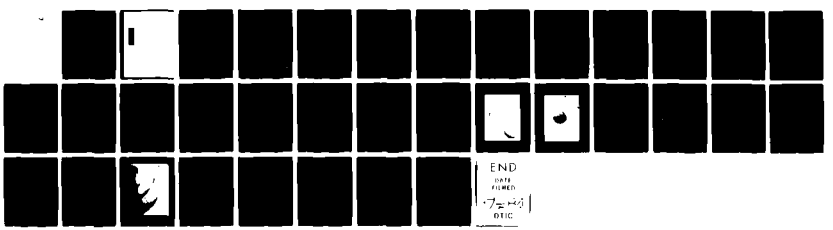

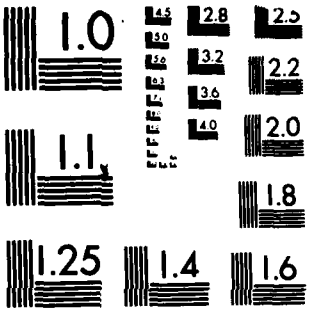

AD-A141 533

SECURITY CLASSIFICATION OF THIS PAGE

REPORT DOCUMENTATION PAGE

1a REPORT SECURITY CLASSIFICATION UNCLASSIFIED	1b RESTRICTIVE MARKINGS
2a SECURITY CLASSIFICATION AUTHORITY	3 DISTRIBUTION/AVAILABILITY OF REPORT
2b DECLASSIFICATION/DOWNGRADING SCHEDULE	Approved for public release; distribution unlimited.
4 PERFORMING ORGANIZATION REPORT NUMBER(S) NRL Memorandum Report 5292	5 MONITORING ORGANIZATION REPORT NUMBER(S)
6a NAME OF PERFORMING ORGANIZATION Naval Research Laboratory 6b OFFICE SYMBOL (If applicable)	7a NAME OF MONITORING ORGANIZATION
6c ADDRESS (City, State and ZIP Code) Washington, DC 20375	7b ADDRESS (City, State and ZIP Code)
8a NAME OF FUNDING/SPONSORING ORGANIZATION 8b OFFICE SYMBOL (If applicable)	9 PROCUREMENT INSTRUMENT IDENTIFICATION NUMBER
8c ADDRESS (City, State and ZIP Code)	10 SOURCE OF FUNDING NOS. PROGRAM ELEMENT NO: 61153N; PROJECT NO: RR0340642; TASK NO: ; WORK UNIT NO: 41-0939-04
11 TITLE (Include Security Classification) OVERVIEW OF ULTRAVIOLET REMOTE SENSING OF THE IONOSPHERE	
12 PERSONAL AUTHOR(S) R.R. Meier	
13a TYPE OF REPORT Interim 13b TIME COVERED FROM TO	14 DATE OF REPORT (Yr., Mo., Day) April 12, 1984 15 PAGE COUNT 33
16 SUPPLEMENTARY NOTATION	
17 COSATI CODES FIELD / GROUP / SUB. GR	18 SUBJECT TERMS (Continue on reverse if necessary and identify by block number) Ultraviolet; Ionosphere; Remote sensing

19 ABSTRACT (Continue on reverse if necessary and identify by block number)

Operational requirements in many areas of the Department of Defense identify the need for ionospheric monitoring and forecasting. Properties of the ionosphere can be sensed remotely on a global scale, by observing naturally-occurring ultraviolet emissions generated by photochemical and ionization processes, especially in the F-region. An overview of the field is presented in this report and the various issues are discussed in the context of recent observations of ionospherically-related UV emissions. Day, night, and auroral phenomena are considered separately, due to fundamental differences in the physical and chemical processes involved. It is concluded that the concept of global ionospheric remote sensing shows subetantial promise. The most pressing need is to expand the data base to cover the full range of geographic, local time, and solar and geomagnetic conditions.

20 DISTRIBUTION/AVAILABILITY OF ABSTRACT UNCLASSIFIED UNLIMITED ☒ SAME AS RPT ☐ DTIC USERS ☐	21 ABSTRACT SECURITY CLASSIFICATION UNCLASSIFIED
22a NAME OF RESPONSIBLE INDIVIDUAL R. R. Meier	22b TELEPHONE NUMBER (Include Area Code) (202) 767-2404 22c OFFICE SYMBOL Code 4140

DD FORM 1473, 83 APR EDITION OF 1 JAN 73 IS OBSOLETE

SECURITY CLASSIFICATION OF THIS PAGE

CONTENTS

I. INTRODUCTION 1

II. SENSING OF THE DAYTIME IONOSPHERE 5

III. SENSING OF THE NIGHTTIME IONOSPHERE 9

IV. AURORAL IONOSPHERE 14

V. SUMMARY 15

REFERENCES 29

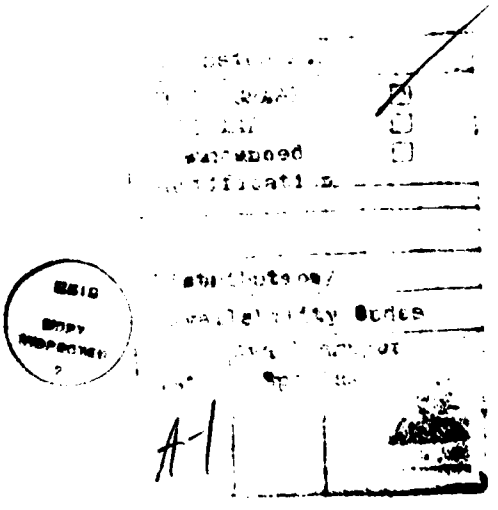

OVERVIEW OF ULTRAVIOLET REMOTE SENSING OF THE IONOSPHERE

I. INTRODUCTION

The need for ionospheric assessment and forecasting is recognized in many areas of the Department of Defense. Specific operational requirements call for monitoring of the ionosphere on a global scale. In particular for the Navy, the relevance of ionospheric sensing to C^3I, Space and other areas is described in CNR/CND Naval Needs for POM 85. Specific areas addressed by ionospheric research are communications, surveillance, intelligence, and navigation. In a memorandum (8 June 1982) the Chief of Naval Operations advocated the role of the Navy in space, and the Chief of Naval Research endorsed the concept in his cover memo of 2 July 1982. For the Air Force, operational needs are described by MAC 02-80 (SON) for Ionospheric Sensing (IONS) which calls for total electron content observations, information on phase scintillation and global electron density profiles. Requirements for the information extend to all geophysical conditions, from the perturbed auroral zone to the scintillating equatorial ionosphere. Many operational requirements would be met if a system were available to provide rapidly the needed ionospheric information on a global scale.

At the present time ionospheric monitoring systems consist of either 1) in situ sampling systems, which measure electron and ion densities by means of rocket or satellite payloads, or 2) active sounding systems, such as top- or bottom-side sounders, or beacons. While these systems can provide electron density profiles or total electron content (TEC), they suffer from the deficiency that the measurement is only a "snapshot" or at best, a tracing along a satellite track or a sampling at one point on the earth of ionospheric conditions. These systems do not have the capability

Manuscript approved December 12, 1983.

of providing prompt monitoring of the ionosphere on a global scale.

For rapid ionospheric monitoring and forecasting requirements, the "ideal" system would consist of high altitude passive detectors, perhaps some at synchronous orbit, which could provide global images of the electron density or TEC. There is no way to accomplish this directly. However, oxygen ions in the F-region are known to emit ultraviolet (UV) radiation or to interact photochemically with ionospheric constituents to produce radiation that can be sensed remotely. The F-region is a neutral plasma, and since O^+ is the dominant ion there, the electron density equals the oxygen ion (O^+) density (from below 200 to above 500 km). Thus, a measurement of O^+ yields the electron density.

Figure 1 illustrates the concept of far ultraviolet remote sensing of ionospheric weather, much the same as is provided presently by visible and infrared imaging systems which monitor low altitude (tropospheric) weather. Two levels of information, qualitative and quantitative, would be available from such an ionospheric system. Qualitatively, the response of the ionosphere to solar activity and resultant magnetic storms would be seen, regions of irregularities and patchiness could be identified, and the extent of the auroral ovals and magnetospheric energy dumping regions would be monitored. Quantitative information in the form of diagnostic plasma spectroscopy and modelling would provide the electron density, height information, and data on the neutral composition.

UV remote sensing of the ionosphere is now state-of-the-art for several reasons. During the last several years laboratory measurements have

been made of the atomic processes which produce the UV emissions. Knowledge of the atomic parameters determined from these measurements is critical in order to relate optical observations to ionospheric density profiles. Quality instrumentation is now available which can perform UV remote sensing measurements to high absolute accuracy (although in some cases only relative measurements are required). Sophisticated models have been developed which now allow determination of quantitative ionospheric (and neutral atmospheric) parameters from optical observations. Now is the appropriate time to exploit the potential of UV remote sensing.

Optimum observing scenarios have not been defined. At the present time, the most urgent need is for more data. On a global scale, spectrally broad-band images have been obtained by the NRL camera carried to the lunar surface on Apollo-16 (Carruthers and Page, 1976) and by Dynamics Explorer (Frank et al., 1982). While much qualitative information is available from such images, except for a few special observing conditions, the spectral purity required for diagnostic spectroscopy is not available. Furthermore, no images have been obtained for wavelengths below 100 nanometers (nm), the spectral region which is rich in O^+ emission lines.

Limited line-of-sight observations have been obtained from a few rocket and satellite missions. However, better spatial resolution and more extensive observations with high sensitivity instrumentation are required to fully explore the UV sensing capability. It is possible to achieve many ionospheric assessment objectives using spacecraft at altitudes below synchronous orbit; perhaps a combination of observing platforms would be optimum.

Specific application of such remote sensing systems to communications is primarily in prompt, worldwide measurement of the F-region electron density, with special emphasis on assessment and forecasting. Total electron content could be determined by measurement of several complementary ionospheric and thermospheric emissions. Other systems, such as over-the-horizon radar, which utilize the high frequency (HF) spectrum, would be supported by knowledge of ionospheric electron density on a wide geographical scale across the northern hemisphere. In the intelligence area, knowledge of atmospheric and ionospheric conditions over hostile areas would be obtained. In the nuclear environment, not only detection but also knowledge of atmospheric and ionospheric effects and their evolution following an event would be provided by a UV monitoring system. Assessment of atmospheric conditions affecting drag of navigation satellites and reentry vehicles, and the use of UV limbs and discrete sources for autonomous navigation are both potential applications of UV remote sensing.

Surveillance aspects of the UV bear special mention. Low background and high sensitivity of UV instrumentation offer attractive alternatives which would complement existing systems. Precise targeting is also possible in the UV.

Ionospheric and neutral ionospheric data obtained from UV sensing systems would be invaluable scientifically. Responses to solar and magnetospheric perturbations of the ionosphere would be studied quantitatively. The resulting dynamical effects propagating to lower latitudes could be studied. Phase and amplitude separation would be achieved. Limb scans would give top side scale heights and therefore

temperatures. Compositional changes would be determined.

In this report, examples of UV observations of the ionosphere and upper atmosphere are presented to provide background information and to define current state-of-affairs. Separate discussions are made of daytime, nighttime, and auroral conditions, since the physical and chemical processes leading to radiation production are different in each case. Finally, specific issues are summarized regarding approaches to the development of an ionospheric remote sensing capability.

II. SENSING OF THE DAYTIME IONOSPHERE

The far ultraviolet (FUV: 100-200 nm) and extreme ultraviolet (EUV: 10-100 nm) are ideal spectral regions for inferring the high altitude atmospheric and ionospheric conditions, not only because characteristic emission lines of the ions, atoms, and molecules reside in this spectral region, but also because background radiation is low. Molecular oxygen absorbs FUV radiation below about 100km, and O, O_2 and N_2 absorb strongly in the EUV. Thus, Rayleigh, aerosol, and cloud scattering of sunlight are negligible. The near-earth UV radiation field is illustrated in Figure 2, which shows a UV image of the earth taken with the NRL S-201 camera experiment during the Apollo-16 mission (Carruthers and Page, 1976). The sun is shining from the lower left. The wavelength band is 123-150 nm. The day side of the ionosphere is overexposed. Auroral zones are seen in perspective at the north and south poles. The arcs present in the tropical ionosphere at night are due to the combined effects of electric fields and

winds redistributing the plasma. Weak emission is also present at midlatitudes at night. Nighttime conditions will be discussed in the next section.

While the day side of Figure 2 is overexposed, shorter exposure photographs show structure in the auroras, and broad, diffuse emission from the sunlit disk. The broad band (123-150 nm) consists primarily of atomic oxygen and molecular nitrogen emissions. (See Figure 3.) Had the images been monochromatic (at specific wavelengths), differences in the global distributions of O and N_2 would have been evident in images with lower exposure times.

Dayglow spectra observed from sounding rockets (Meier et al., 1980) are shown in Figure 3. The center panel shows the spectral composition over the wavelength range covered by the image of Figure 2. A spectral synthesis model is shown as the dashed curve. The model is able to reproduce the data nearly exactly, demonstrating that the major emission features have been identified and their brightness levels understood. An extensive set of satellite observations of this band have been reported by Huffman et al.,(1980). The mid-ultraviolet (MUV) spectrum on the right was actually taken in an aurora, although the dayglow should be similar (Beiting, and Feldman, 1979). The lower panel demonstrates high precision in which MUV bands of molecular nitrogren and nitric oxide can be modelled.

The left panel displays a spectrum of the EUV, showing the richness of O^+ emissions below 100 nm (Feldman et al., 1981). The brightest feature is the resonance line at 83.4 nm (834 Å), which is off scale in the figure.

This feature is the prime candidate for monitoring the F-region O^+ (and therefore electron) density during the day. Other O^+ emissions are weaker, but could provide important supplementary information. Details of how this is done are described next.

O^+ radiation at 83.4 nm is produced in the ionosphere when oxygen atoms are ionized by sunlight. Some of the ions are in excited states which promptly radiate in the EUV, most strongly at 83.4 nm. Energetic electrons in the ionosphere collide with O atoms, also contributing to the 83.4 nm production rate. The abundance of oxygen ions is sufficient to cause multiple scattering of 83.4 nm photons before they can escape from the atmosphere (or reach a detector). Thus, optically thick, multiple scattering models are required in order to extract information from observations of the EUV radiation. The modelling procedure is shown schematically in Figure 4. The degree of sophistication of the models is high. The model of sunlight interaction with the ionosphere to produce energetic electrons includes energy loss through excitation of some 50 atomic and molecular states of atmospheric gases. Some of the models which are used for intensity computations allow for multiple scattering of photons in an optically thick, spherical, non-isothermal, inhomogeneous atmosphere. All phases of the modelling have been completed at NRL and have been applied to rocket and satellite observations at 83.4 nm (and many other emission features).

An example of the altitude dependence of the O^+ 83.4 nm emission rate measured in the rocket spectrum of Figure 3, is shown in the left panel Figure 5. The instrument line-of-sight was horizontal. The solid line

shows the result of the NRL analysis. The O^+ density which best fit the data is shown in the right panel. Ground truth was obtained from a simultaneously operating, ground-based ionosonde, which measured bottom-side and peak electron densities in excellent agreement with the O^+ density shown.

Evaluation of use of 83.4 nm as a diagnostic of ionospheric conditions is proceeding at NRL. Parametric studies show that limb scans and imaging could yield the O^+ density profile. In principle, th atio of 83.4 nm to an optically thin line, such as 61.7 nm, yields the (and electron) column content along the line-of-sight. These models are ' ıg applied to limited data sets from the NRL Space Ultraviolet Radiation E. .onment (SURE) experiment, which was flown on the Shuttle (STS-7) in June 1983, and the University of California EUV spectrometer experiment on STP 78-1. Again, the preliminary results are very encouraging. For more extensive synoptic observations from satellites, it is anticipated that the iterative modelling scheme shown in Figure 4 would be replaced by a more sophisticated technique.

The neutral atmospheric composition can be obtained using FUV spectral data. The series of papers by the NRL, Johns Hopkins University and Goddard Space Flight Center have demonstrated that accurate atmospheric parameters can be extracted from such data (Meier et al., 1980; Anderson et al., 1980 a, b; Feldman et al., 1981). It is particularly important to know the neutral composition since 83.4 nm radiation can be absorbed by the atmosphere at lower altitudes. Molecular nitrogen can be monitored by emissions between 120 and 150 nm. The relative line strengths provide a

measure of O_2, since its absorption is different for the different N_2 bands. Atomic oxygen can be observed through its bright lines at 130.4 and 135.6 nm (shown off-scale in Figure 3).

Knowledge of the atomic oxygen density is an important supplement to O^+ 83.4 nm observations, since it plays a central role in the production of the radiation. As an example of an atomic oxygen measurement, the results from the Aerospace Corp. D-sensor on the DMSP-F4 spacecraft were chosen (Newman et al., 1983). Figure 6 shows a sketch of the limb-scanning geometry. Data at 135.6 nm are shown in the left panel of Figure 7 along with the best fit model. The atomic and molecular oxygen densities found from NRL analyses of the data are given in the right panel. Error bars on the data give the statistical uncertainty. Current instrumentation could reduce the statistical uncertainty by more than an order of magnitude.

To summarize, the O^+ 83.4 nm line is the principal diagnostic feature to provide ionospheric observability during the day. Other EUV lines can provide additional information for verifying the O^+ 83.4 results. F-region ion and therefore electron densities and scale heights, in principle, can be extracted from such data. Simultaneous observations of the neutral atmospheric composition can be obtained from the FUV band, and are important for analyzing O^+ data due to the central role of O in 83.4 nm production, and atmospheric absorption by O, O_2 and N_2.

III. SENSING OF THE NIGHTTIME IONOSPHERE

The earth's ionosphere is produced primarily by solar photoionization

during the day. At night, species ionized during the day recombine, resulting in a lower plasma density. Recombination of O^+ at night leads to UV optical emissions which may be observed from satellites. While the signal levels are much weaker than during the day, they are detectable nonetheless and can serve as diagnostics of ionospheric conditions. Also, the photochemical theory is much simpler at night. In this section, the photochemical theory is discussed along with several examples of its application to ionospheric remote sensing.

There are two main processes which lead to the production of radiation from the nighttime ionosphere. The first involves recombination of O^+ with ambient electrons:

$$e + O^+ \rightarrow O + \text{UV radiation}$$

The intensity from this process is given by

$$I = \sigma \int n(e)\, n(O^+)\, ds \qquad (1)$$
$$= \sigma \int n^2(e)\, ds$$

in the F-region. Here, is the radiative recombination coefficient and n is the density of the indicated species. The integral is carried out along the line-of-sight. (There is a small correction for $O^+ + O^- \rightarrow 2O +$ radiation, but often this can be neglected entirely.) For a detector viewing vertically downward from above the ionosphere, I is essentially proportional to the square of the electron density at the F_2 peak. The proportionality is given by

$$I = \sigma \; e \; H \; (n_{max})^2 \qquad (2)$$

where e is the base of the natural logarithms, H is the atomic oxgyen scale height, and n_{max} is the F_2 electron density peak (Meier and Opal, 1975). Tinsley and Bittencourt (1975) verified theoretically this simple description with a more elaborate model of the tropical ionosphere. The UV emissions produced in this process are at 91.1, 130.4 and 135.6 nm. They were discovered first in the nighttime ionosphere with the NRL experiment aboard the NASA OGO-4 spacecraft (Hicks and Chubb, 1970). The validity of the proportionality between I and $n^2(e)$ was proven by Meier and Opal (1973) who correlated UV data from OGO-4 with overpasses of ground-based ionosondes.

Later work involving a collaboration between Goddard Space Flight Center and NRL exploited the remote sensing potential of the OGO-4 experiment (Chandra et al., 1975). Figure 8 shows an example of their study; contours of electron density at the F_2 peak are plotted on a geographic map for a local time of 2146. Data from a two day period were accumulated to make this map. The relationship of n(e) to the magnetic dip equator is clearly seen. The electron density maximized on either side of the equator due to the effect of electric fields which move the plasma vertically upward. The plasma then flows down along higher field lines, resulting in net transport to higher latitudes. Since the radiative recombination is proportional to the square of the electron density, arc-like structures are formed in the F-region on both sides of the magnetic equator and are clearly seen in the Apollo-16 photograph (Figure 2).

An alternative global view of the instantaneous F-region electron density can be obtained from the Apollo-16 results. The photograph in Figure 2 was digitized, converted to absolute brightness, and then to electron density via equation (2). The result is shown in Figure 9. While the electron density contours are not exact due to approximate corrections for scattered light, nonetheless Figure 9 serves to illustrate the potential of high altitude remote sensing of the ionosphere on a global scale.

Other examples of UV sensing of the nighttime ionosphere are shown in Figure 10. The NRL experiment on board the STP 72-1 satellite observed both the 911 nm (800-1050 Å in the figure) and the 130.4 and 135.6 nm (1220-1400 Å) emissions (Anderson et al., 1976). The figure shows sub-satellite intensities for four individual passes. The high-sensitivity photometers showed that weak signals of less than a Rayleigh (1R = 10^6 photons cm^{-2} s^{-1} (4π steradian)$^{-1}$ = 79577 photons cm^{-2} s^{-1} str^{-1}) are observable.

Altitude distributions of the electron density could have been obtained in the above emissons if limb scans had been made with high spatial resolution. However, altitude information is still available if other plasma emission features are measured. This is the point of the second important diagnostic process:

$$O_2^+ + e \rightarrow 2O + \text{radiation}.$$

The bright red line of atomic oxygen at 630 nm is one of the emissions produced. Since O_2^+ is produced via

$$O^+ + O_2 \rightarrow O + O_2^+,$$

in the F-region, the red line intensity is proportional to the product of the O_2 and the electron (O^+) densities. By combining UV observations to obtain the electron density at the F peak with red line observations and a model of the O_2 density, the altitude where the maximum electron density occurs can be determined. (Low altitude quenching of the red line should be taken into account for accurate heights.) A model of this procedure was developed by Chandra et al. (1975). Application to OGO-4 data is shown in Figure 11. (The Goddard group measured the red line simultaneously with the NRL UV measurements.) These altitudes correspond to the electron densities in Figure 8. A clear trend toward higher altitudes near the equator is seen, although some asymmetries are seen. Asymmetries are attributed to meridional winds. Bittencourt and Tinsley (1976) developed a theory which allows the determination of wind speeds from simultaneous measurements of the 630 and 135.6 nm emissions. Bittencourt et al. (1976) actually applied the theory to OGO-4 data. Thus, if the right combination of ionospheric emission features is measured, information about not only the electron density, but also the height can be obtained from line-of-sight observations and images.

The above discussion applies to the normal, unperturbed ionosphere. Under Spread-F or other disturbed conditions, the simple theory breaks down. Still, disturbed regions should show up qualitatively in contrast to the surrounding quiet ionosphere. Preliminary calculations suggest that Spread-F behavior should have a different optical signal. No optical data exist for such disturbances. Spectroscopic exploration of disturbed

conditions is urgently needed, along with limb scans and images to study the observability.

IV. AURORAL IONOSPHERE

Remote optical sensing data from the auroral ionosphere has not yet been analyzed to the same degree of detail as that at mid- and low-latitudes. The UV offers the ability to study energy deposition and morphology, as first was shown in the pioneering work on OGO-4 data by Chubb and Hicks (1970), and most recently on Dynamics Explorer (Frank et al., 1982). In fact detailed information about the neutral composition, at least in steady, diffuse auroras, and characteristics of the primary precipitating electrons can be obtained using UV spectroscopy (Meier et al., 1982; Strickland et al., 1983). From such data it is possible to use photochemical models of the ionosphere to compute the electron density, but the reliability of such models needs to be verified experimentally.

Utility of the O^+ 83.4 nm emission depends upon the degree of ionization. If the electron density is significantly below 10^5 cm $^{-3}$, multiple scattering will be infrequent and intensity measurements will give only the ionization rate of atomic oxygen. However this knowledge may be sufficient to greatly improve the reliability of auroral ionospheric models. Radiative recombination lines at 91.1, 130.4 and 135.6 nm will be masked by energetic electron impact excitations (as also is the case during the day). Auroral photochemistry involves a broad range of excitation processes. Clearly an extensive investigation needs to be made to identify relevant emission lines for the most direct determination of the plasma composition.

It should be noted that the UV offers a significant advantage over the visible and infrared. The background is low so that observations can be made both day and night. Furthermore, the emission features are relatively uncluttered, unlike the myriad molecular bands present at longer wavelengths.

V. SUMMARY

In this report I have described the various aspects and the potential of remote sensing of the ionosphere and have reviewed the current state of knowledge of relevant observations and models. The major neutral and ion emission lines have been identified in the extreme and far UV spectrum. The excitation mechanisms for most of the emissions have been identified and in most cases, physical models are available for data interpretation.

The most critical need is to expand the data base. High spatial resolution limb scans are essential to verify the expectations of the models and to define the optimum set of emission features to be used in an ultimate systems concept. This is especially true in the EUV below 100 nm, where such data are virtually nonexistent. Data are needed over a wide range of geographic regions, local times, and geomagnetic activity. The optical observability of regular and anomalous ionospheric phenomena needs to be established. The next phase of experimentation should be directed at proof-of-concept. "Ground truth" should be an integral part of any program.

Ultimately, a high altitude imaging network would be extremely valuable

for systems use in providing prompt global ionospheric conditions. Low altitude spacecraft such as DMSP can provide satellite-track images and local limb scans. While not an "either/or" situation, the relative merits of low- and high-altitude remote sensing should be assessed. Definition of optimum instrumentation for systems use must be considered a major planning objective. Certainly broad-band images such as those obtained on Apollo-16 or Dynamics Explorer provide important contributions. But ultimately monochromatic images will be required. With separate images of N_2, O, and O^+ emissions, quantitative behavior of ionosphere could be discerned. Relative variations in the emissions could be observed as the ionospheric composition changes in response to solar, geomagnetic or man-made perturbations.

Much of the interpretive modelling has been developed at NRL over the past decade. These include physical models of the excitation and emission processes, of the ionospheric photochemistry, and the radiative transport models which link observables to physical parameters. These models have been designed mostly as pioneering efforts to interpret observations of emission features on a limited scale. The various algorithms need to be optimized for prompt provision of ionospheric parameters from UV observations. Deconvolution, precomputation, iterative, and other numerical techniques should be developed, without sacrificing the physical integrity of the models.

Most "semi-operational" ionospheric models are empirical in nature and are driven by such parameters as the solar 10.7 cm or X-ray fluxes, geomagnetic indices, and data from ionosonde stations. It is expected that

the accuracy of such models would be upgraded significantly if the empirical models were based on prompt, actual measurements of ionospheric density. Furthermore, although areas of the ionosphere such as the E-region are not observed directly when O^+ is not the dominant ion, the fact that UV sensing gives not only the F-region density, but also the neutral composition and ionization rates during the day, and monitors UV ionization sources at night (Strobel, Opal and Meier, 1980), simple physical models could be used with confidence to infer the nature of ionospheric-thermospheric characteristics not measured directly.

Finally, remote sensing of the ionosphere in the UV offers the opportunity to provide a global monitoring capability which cannot be obtained any other way.

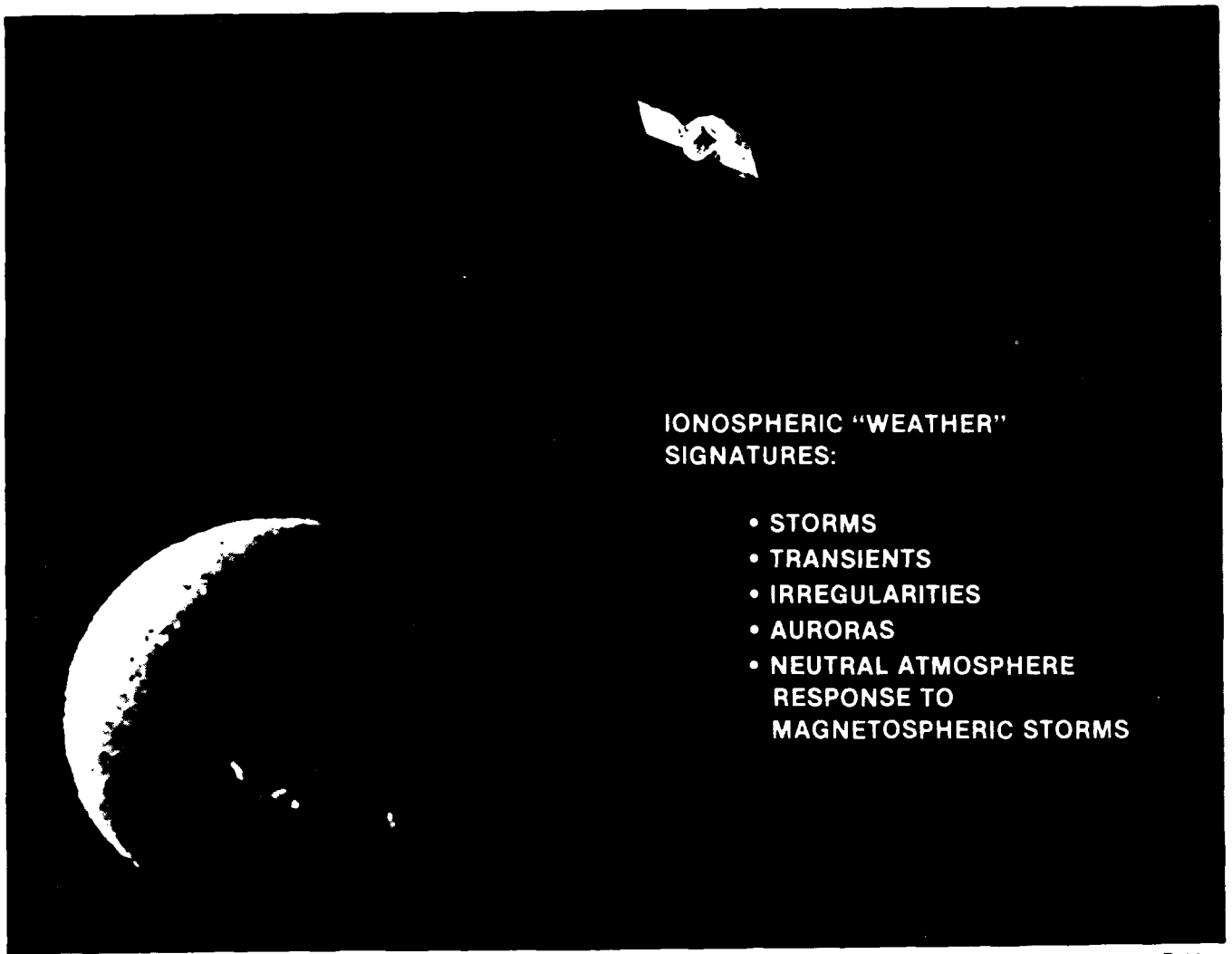

Fig. 1 — Illustration of global monitoring concept. The image consists of a broad band (123-165 nm) polar view of the earth which was constructed from successive scans with a narrow field-of-view photometer on the *Dynamics Explorer* satellite (L. Frank, private communication).

76604(4A)

Fig. 2 — Far UV (123-150 nm) photograph of the earth from Apollo-16. The solar direction is to the lower left and the dayglow (overexposed) covers the left side of the disk. The auroral ovals are seen in projection at the north and south. The bands at night originate from radiative recombination of $O^+ + e$ in the tropical ionosphere. The bright spots away from the earth are stars.

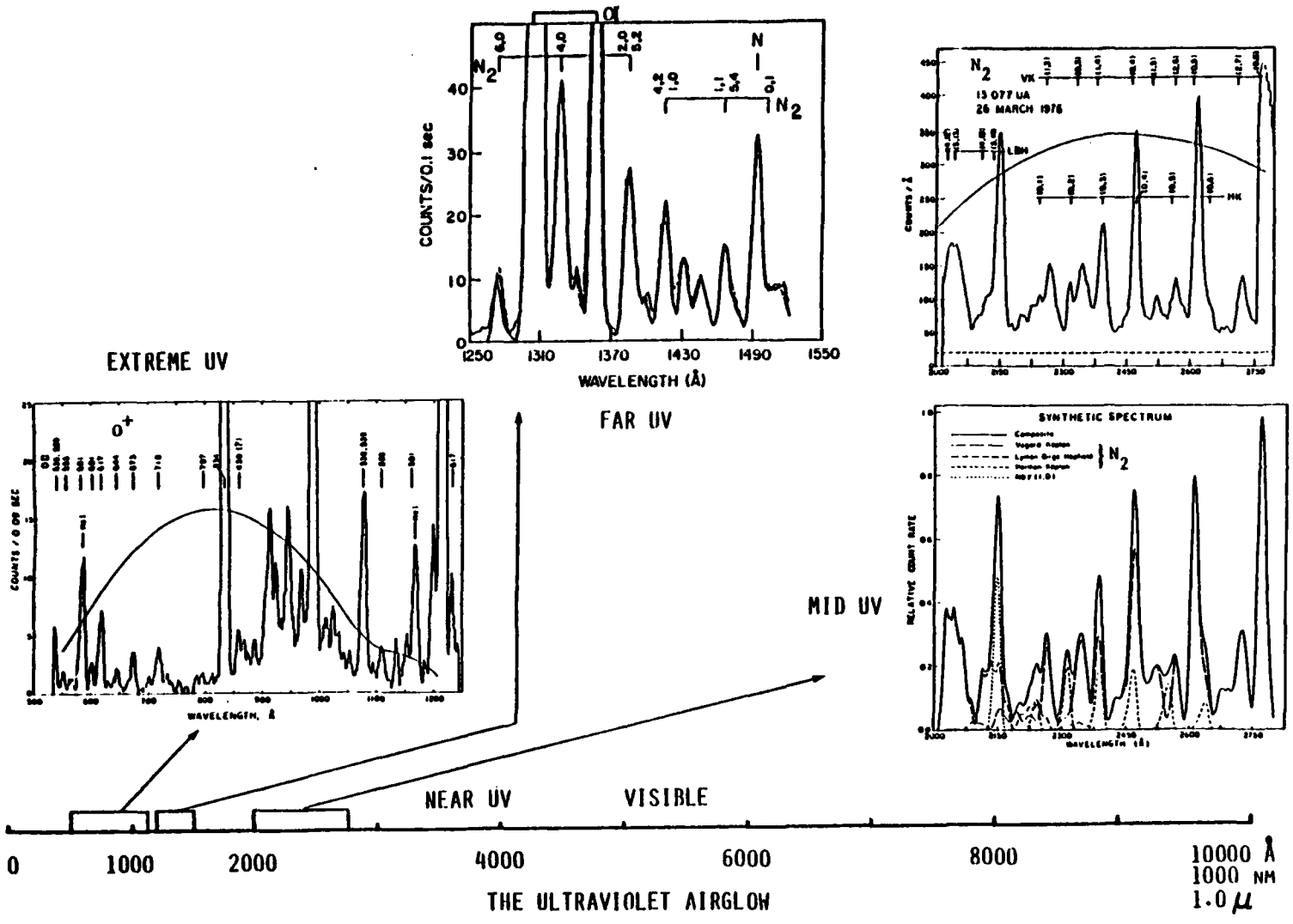

Fig. 3 — Examples of EUV, FUV, and MUV dayglow spectra. The broad lines across the EUV and MUV spectra indicate instrumental responses. Model spectra are shown for MUV (lower right panel) and FUV (dotted lines).

EXAMPLE OF IONOSPHERIC PLASMA DIAGNOSTIC MODELLING

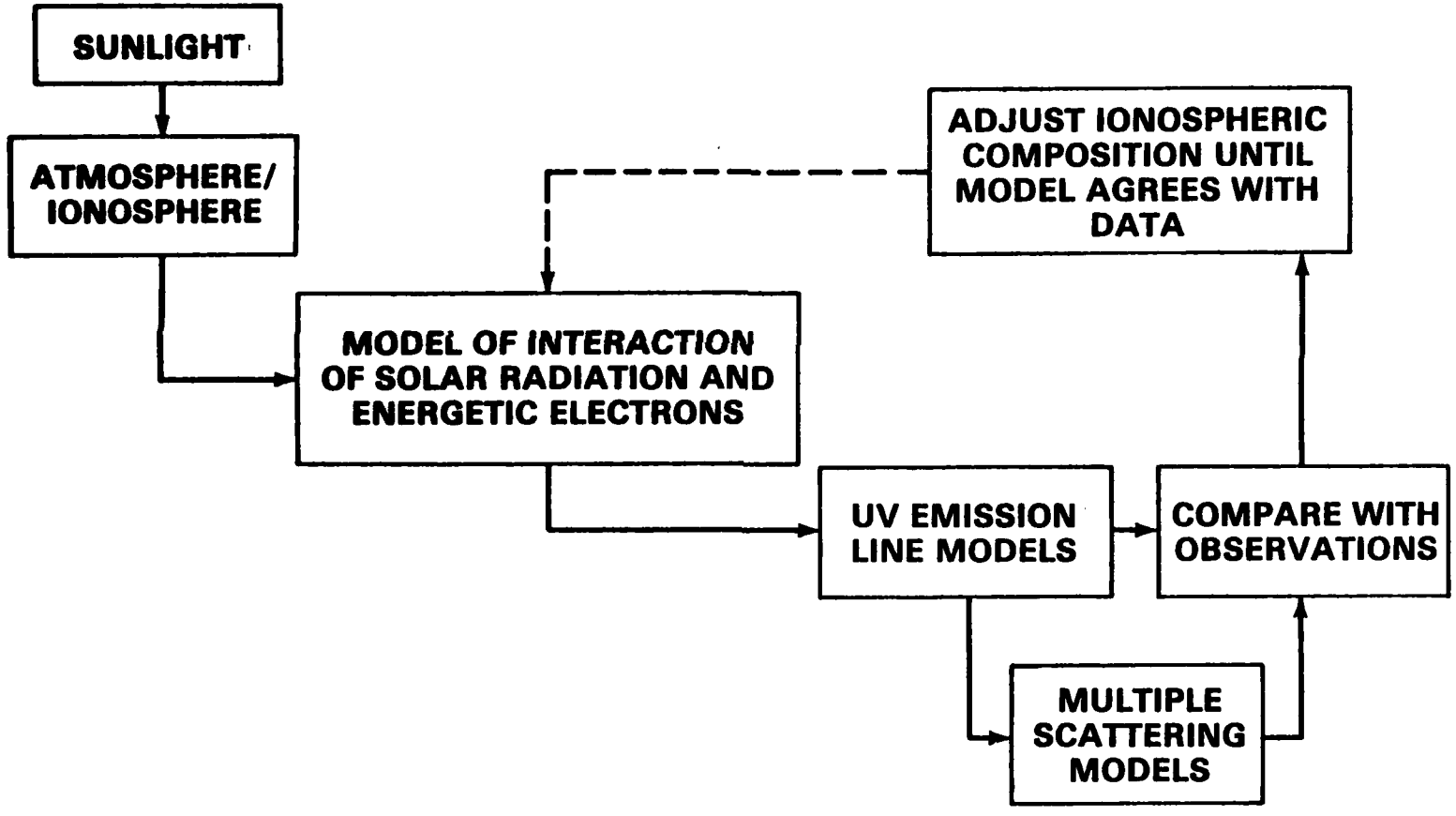

Fig. 4 — Typical procedure for data analysis

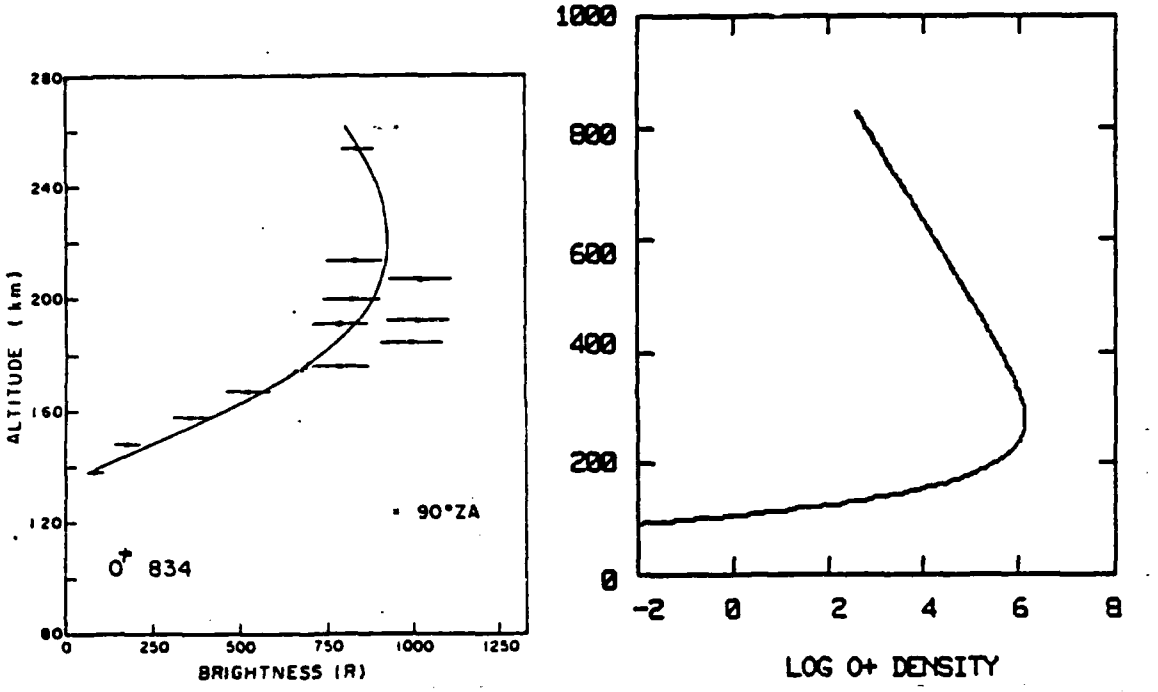

Fig. 5 — 0^+ determination from NRL anaylsis of 1978 JHU/NASA-GSFC dayglow rocket observations of 0^+ 834 Å (In the F-region, the electron density equals the 0^+ density).

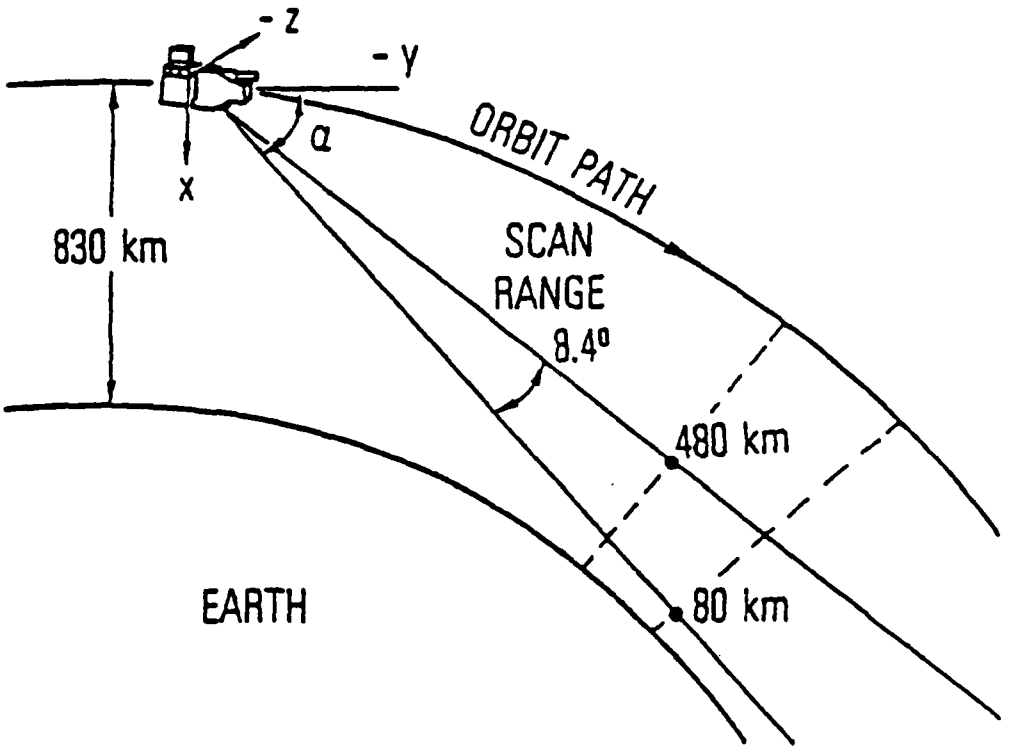

DMSP-F4 (1979) UV LIMB SCANNER

Fig. 6 — Sketch of the Aerospace limb scanning instrument operation on the DMSP F-4 spacecraft

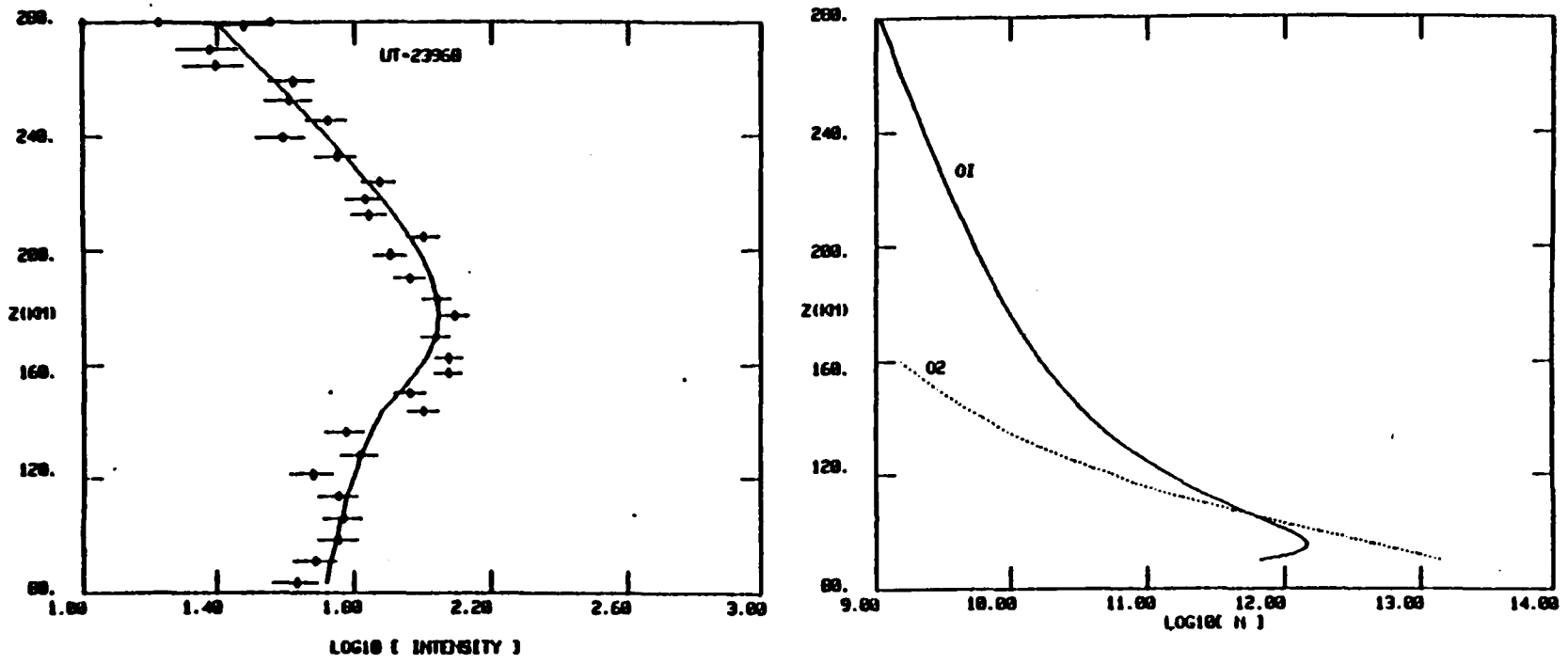

OXYGEN DENSITIES

FROM DMSP-F4 UV DATA

Fig. 7 — Typical limb scan of the atomic oxygen 135.6 nm emission (left pause) observed by the Aerospace experiment on DMSP F-2, and molecular oxygen densities derived from the observations.

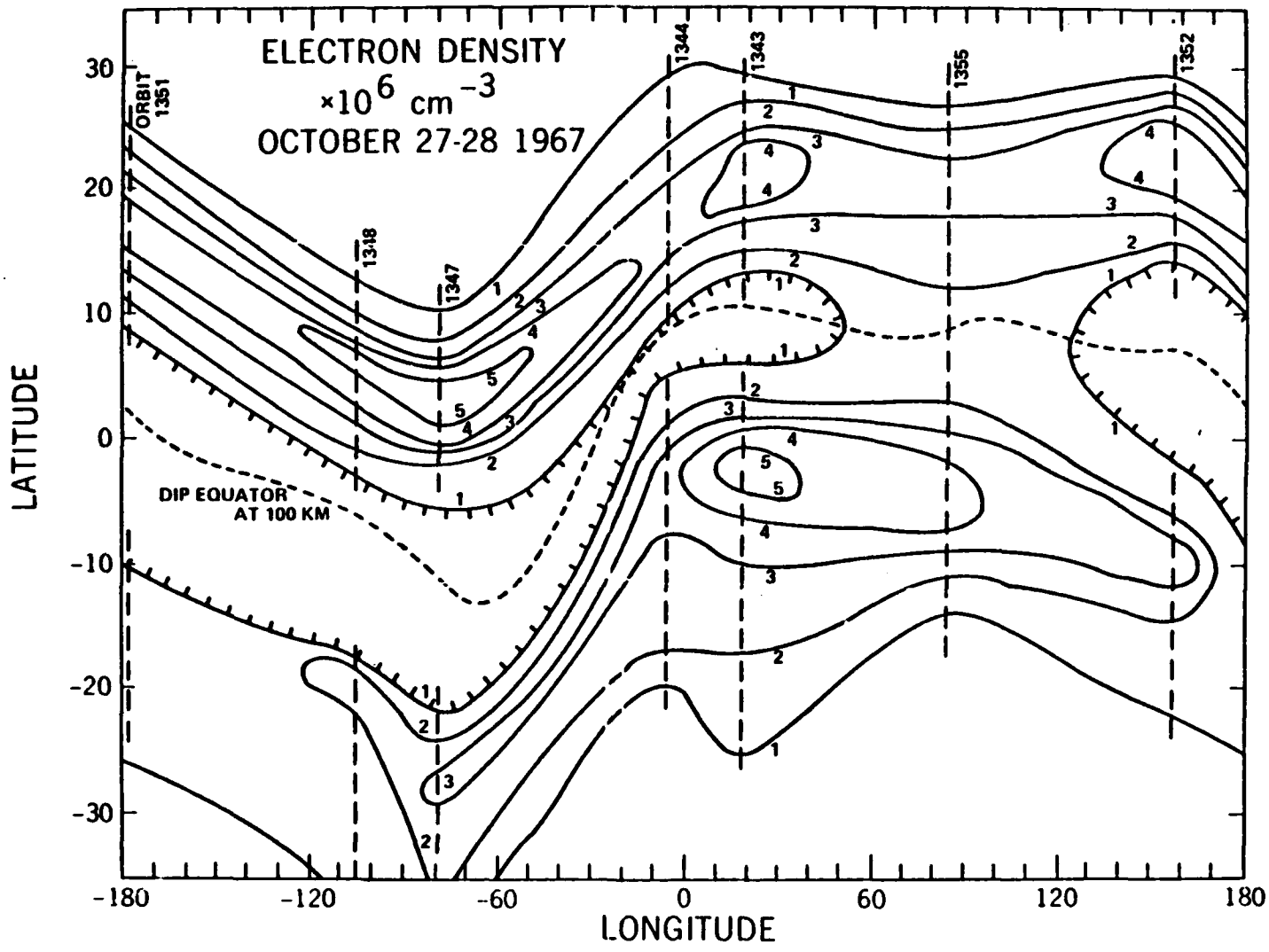

Fig. 8 — Electron densities at the F_2 peaks derived from OGO-4 observations of the oxygen 135.6 nm recombination emission. The maps were constructed over a two day period at a local solar time of 2146. Contours are labelled in units of 10^6 electrons cm^{-3}. Ticked area are below the OGO-4 instrument sensitivity.

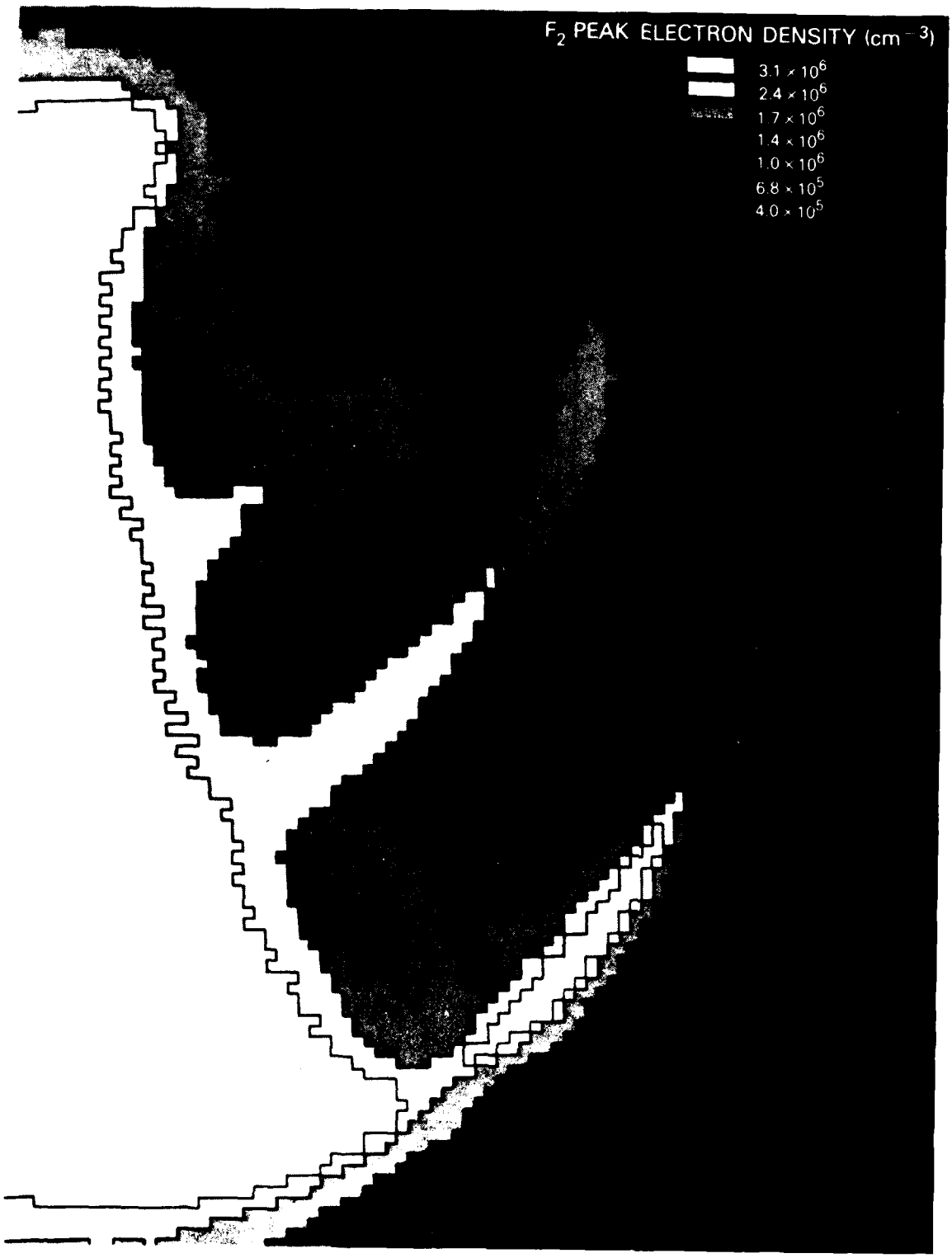

77759(3A)

Fig. 9 — Contours of peak electron density (electrons cm^{-3}) derived from the Apollo-16 photograph in Fig. 2. Note that the dayside image is overexposed.

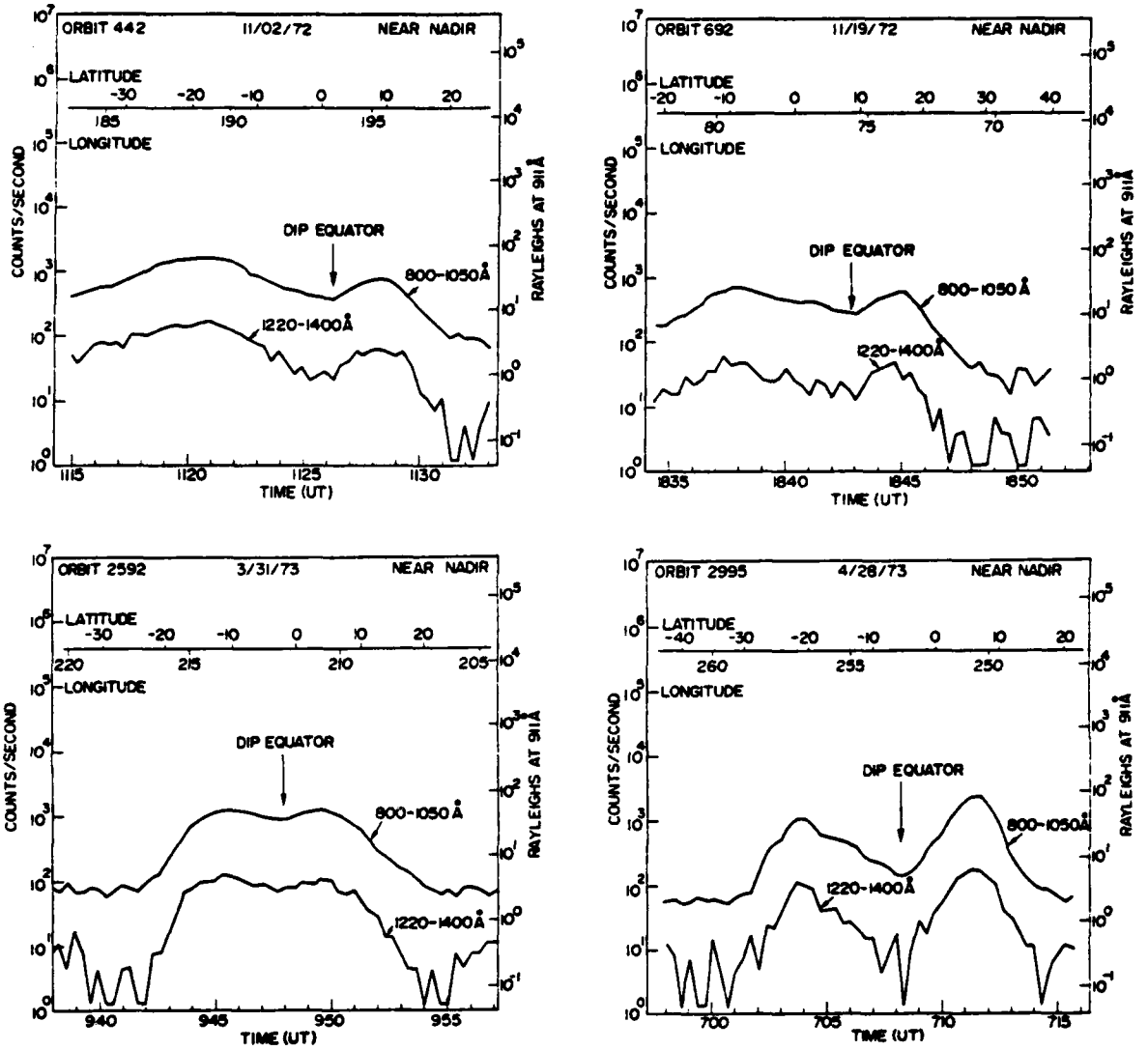

Fig. 10 — Four passes showing observation of oxygen recombination emission at 91.1 (800-1050 Å) and 130.4 and 135.6 (1220-1400 Å) nm from the nighttime ionosphere. Data were taken by the NRL experiment on STP 72-1, viewing downward from 740 km.

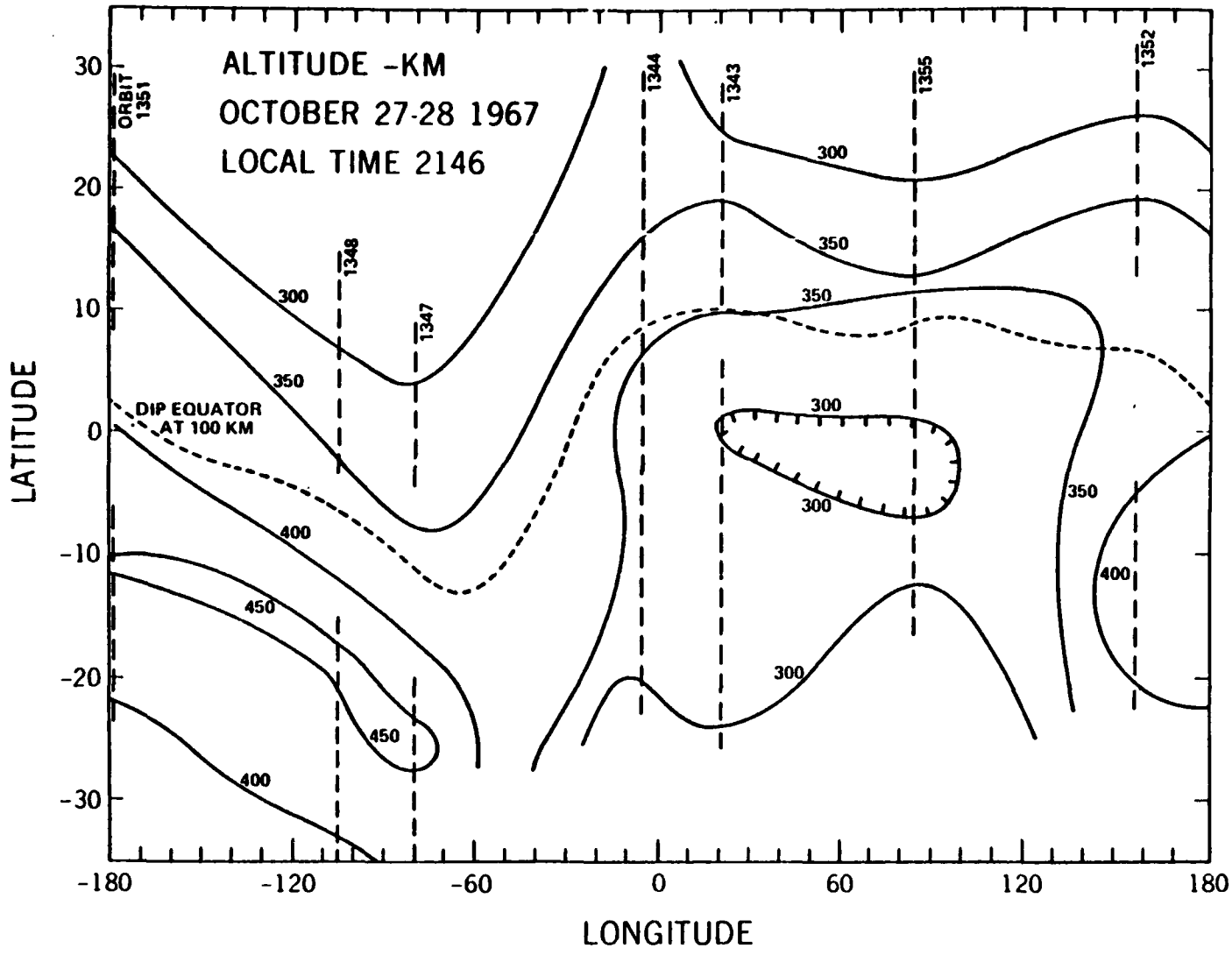

Fig. 11 — Contours of altitudes of the F-region electron density peak, corresponding to the densities in Fig. 8.

REFERENCES

Anderson, D.E., Jr., P.D. Feldman, E.P. Gentieu, and R.R. Meier, The UV dayglow 2, LYα and LYβ emissions and the H distribution in the mesosphere and thermosphere, Geophys. Res. Lett., 7, 529, 1980.

Anderson, D.E., R.R. Meier, P.D. Feldman, and E.P. Gentieu, The UV dayglow 3, OI emissions at 989, 1027, 1152, 1304, and 1356A Geophys. Res. Lett. 7. 1057, 1980.

Anderson, D.E., Jr., R.R. Meier, and C.S. Weller, Observations of far and extreme ultraviolet OI emissions in tropical ionosphere, Planet. Space Sci. 24, 945, 1976.

Beiting, E.J., III, and Feldman, P.D., "Ultraviolet spectrum of the Aurora (2000-2800 Å)", J. Geophys. Res. 84, 1287-1296, 1979.

Bittencourt, J.A., and B.A. Tinsley, Tropical F region winds from OI 1356-and OI 6300-A emissions,1, Theory, J. Geophys. Res. 81, 3781, 1976.

Bittencourt, J.A., B.A. Tinsley, G.T. Hicks, and E.I. Reed, Tropical F region winds from OI 1356-and OI 6300 A emissions, 2, Analysis of Ogo 4 data, J. Geophys. Res. 81, 3786, 1976.

Carrruthers, G.R., and T. Page, Apollo 16 far ultraviolet spectra of the terrestrial airglow, J. Geophys. Res. 81, 1683, 1976.

Chandra, S., E.I. Reed, R.R. Meier, C.B. Opal, and G.T. Hicks, "Remote sensing of the ionospheric F layer by use of OI 6300-Å and OI 1356-Å observations", J. Geophys. Res. 80, 2327, 1975.

Feldman, P.D., D.E. Anderson, Jr., R.R. Meier, and E.P.Gentieu, "The ultraviolet dayglow 4. The spectrum and excitation of singly ionized oxygen", J. Geophys. Res., 86, 3583, 1981.

Frank, L.A., J.D. Craven, J.L. Burch, and J.D. Winningham, "Polar views of the earth's aurora with Dynamics Explorer", Geophys. Res. Lett., 9, 1001-1004, 1982.

Hicks, G.T., T.A. Chubb, "Equatorial aurora/airglow in the far ultraviolet", J. Geophys. Res. 75, 6233, 1970.

Huffman, R.E., LeBlanc, F.J. Larrabee, J.C. and Paulsen, D.E., "Satellite vacuum ultraviolet airglow and auroral observations", J. Geophys. Res., 85, 2201-2215, 1980.

Meier, R.R., D.J. Strickland, P.D. Feldman, and E.P. Gentieu, "The ultraviolet dayglow 1. Far UV emissions of N and N_2", J. Geophys. Res., 85, 2177, 1980.

Meier, R.R., Conway, R.R., Feldman, P.D., Strickland, D.J. and Gentieu, E.P., "Analysis of nitrogen and oxygen for ultraviolet auroral emissions, Journal Geophys. Res., 87, 2444, 1982.

Meier, R.R., C.B. Opal, "Tropical UV arcs: Comparison of brightness with $f_o F_2$", J. Geophys. Res. 78, 3189, 1973.

Newman, A.L., A.B. Christensen, and D.E. Anderson, Jr., "Atomic oxygen density deduced from limb-scans of the UV dayglow", accepted for publication, J. Geophys. Res., 1983.

Strickland, D.J., J.R. Jasperse, and J.A. Whalen, "Dependence of auroral FUV emissions on the incident electron spectrum and neutral atmosphere", J. Geophys Res. 88, 8051-8062, 1983.

Strobel, D.F., C.B. Opal, and R.R. Meier, "Photoionization rates in the night-time E- and F-region ionosphere", Planet, Space Sci., 28, 1027, 1980.

Tinsley, B.A., and J.A. Bittencourt, "Determination of F region height and peak electron density at night using airglow emissions from atomic oxygen", J. Geophys. Res., 80, 2333, 1975.